AUCTORES
Globalize your Research

International Journal of Clinical Case Reports and Reviews
Nan Lu *
Open Access

Research Article

Theoretical investigation on Iodine (III)-Mediated Selective Csp−Csp2 bond Cleavage from Nitrogenation of alkyne with Nitrone Yielding Functionalized [1,4] Oxazinone

Nan Lu *, and Chengxia Miao

College of Chemistry and Material Science, Shandong Agricultural University, Taian 271018, P. R. China.

***Corresponding Author:** Nan Lu, College of Chemistry and Material Science, Shandong Agricultural University, Taian 271018, P. R. China.

Received Date: November 22, 2024 | **Accepted Date:** December 05, 2024 | **Published Date:** December 13, 2024

Citation: Nan Lu, and Chengxia Miao, (2024), Theoretical Investigation on Iodine (III)-Mediated Selective Csp−Csp2 bond Cleavage from Nitrogenation of alkyne with Nitrone yielding Functionalized [1,4] Oxazinone, *International Journal of Clinical Case Reports and Reviews*, 20(5); **DOI:**10.31579/2690-4861/626

Copyright: © 2024, Nan Lu. This is an open-access article distributed under the terms of the Creative Commons Attribution License, which permits unrestricted use, distribution, and reproduction in any medium, provided the original author and source are credited.

Abstract:

Our DFT calculations provide the first theoretical investigation on iodine(III)-mediated selective Csp−Csp^2 bond cleavage of 1-alkynylnaphthol with N-phenyl nitrone. 1-alkynylnaphthol was isomerized to VQM under base NEt3, which underwent [4 + 3] cycloaddition with N-phenyl nitrone affording heptatomic ring. 1,3-rearrangement of N−O vinyl group was determined to be rate-limiting furnishing another heptatomic ring more stable. The ring opening and sequential hydrogen shift gave iminium. The intramolecular 1,4-addition delivered pyrroline through pentacyclic alkene. The intermolecular alcoholysis with MeOH and PhI(OAc)$_2$ pro-vided α-aminoketone. Via oxidative dearomatization and intramolecular cyclization, spirolactam was formed followed by ring opening and ester exchange producing major product [1,4]oxazinone. Alternatively, the in-tramolecular 1,2-addition of O-anion resulted in bridged ring by-product. The positive solvation effect is suggested by decreased absolute and activation energies in solution compared with in gas. These results are supported by Multiwfn analysis on FMO composition of specific TSs, and MBO value of vital bonding, breaking.

Key words: Csp−Csp^2 bond cleavage; iodine(III); [1,4]oxazinone; nitrone; [4 + 3] cycloaddition

Introduction

As privileged method to construct scaffold in drug discovery and add molecular complexity to pharmacophore in chemical synthesis [1,2], reaction of C−C bond cleavage represents attractive strategy with efficient bond reorganization [3,4]. In this aspect, alkynes are most versatile starting materials developed in past decades such as unsaturated, strained Csp−Csp bond easily cleaved with transition metal catalysts, oxidants [5,6] and polar Csp−Csp^3 bond cleaved through radical process or retro-1,2-addition with photocatalysts [7]. However, the cleavage of unstrained Csp−Csp^2 σ-bond is still difficult requiring assistants to generate stable intermediates [8]. Selective Csp−Csp^2 Bond Cleavage: The Nitrogenation of Alkynes to Amides. Up till now, nitrogenation of alkynes was less reported via regioselective Csp−Csp^2 bond cleavage. Only Jiao developed aryl-substituted alkynes with TMSN3 catalyzed by gold(I) to access linear amides [9]. Echavarren discovered sequential cycloaddition to afford tetrazoles [10].

In past decades, 1-alkynylnaphthol was applied as precursor of vinylidene−quinone methide [11] such as Rh-catalyzed azide-internal-alkyne cycloaddition in construction of axially chiral 1,2,3-triazoles [12] and Ir(I)/squaramide cooperative catalysis in asymmetric azide−alkyne cycloaddition [13]. On the other hand, nitrone was demonstrated as various N and O sources in synthesis of novel scaffolds. Luo developed diastereoselective assembly of ten-membered N-heterocycles between two 1,3-dipoles then to access fused N-heterocycles [14]. Xu explored stereoselective photoredox catalyzed (3 + 3) dipolar cycloaddition of nitrone with aryl cyclopropane [15]. Zhou discovered enantioselective oxidative multi-functionalization of terminal alkynes with nitrones and alcohols to assemble chiral α-alkoxy-β-amino-ketones [16]. Li realized stereoselective construction of azepine-containing bridged scaffolds via organocatalytic bicyclization of yne-allenone esters, regio- and enantioselective (3 + 3) cycloaddition of 2-Indolylmethanols [17,18]. Recently, powerful hypervalent iodine(III) compounds have attracted much attention owing to high reactivity in cascade transformation. Wang reported α-functionalization of benzylamides with N-nucleophiles via oxidative Umpolung in synthesis of tetrasubstituted 3,3′-oxindoles and regioselective dearomatization of non-activated arenes [19,20].

In this field, Mo group has achieved cinchonidine-catalyzed synthesis of various oxazabicyclo [4.2.1] nonanones from N-aryl-α, β-unsaturated nitrone and 1-ethynylnaphthalen-2-ol [21]. Another breakthrough was nitrogenation of 1-alkynylnaphthols with N-aryl nitrones and sequential recombination leading to functionalized [1,4]oxazinone mediated by iodine(III) compounds through regioselective Csp−Csp^2 cleavage of alkyne and C=N/N−O bond cleavage of nitrone [22]. [1,4]oxazinone is vital heterocyclic scaffold with extensive pharmacological significance [23,24] also as fluorescence imaging materials [25]. Although a range of [1,4] oxazinones were yielded, many problems still puzzled. There was no report about detailed mechanistic study explaining its vicinal carbon stereocenter with high diastereoselectivity. How vinylidene−quinone methide (VQM) underwent [4 + 3] cycloaddition with N-phenyl nitrone followed by 1,3-rearrangement of N−O vinyl moiety? How pyrroline intermediate was obtained through intramolecular 1,4-addition of iminium intermediate? Why bridged ring by-product resulted from intramolecular 1,2-addition of O-anion was disfavored compared with [1,4] oxazinone via intramolecular cyclization, dearomatization, rearomatization, ring opening of spirolactam and ester exchange? To solve these questions in experiment, an in-depth theoretical study was necessary also focusing on the C−C/C=N/N−O multiple bonds cleavage and recombination.

2 Computational details

The geometry optimizations were performed at the B3LYP/BSI level with the Gaussian 09 package [26,27]. The mixed basis set of LanL2DZ for I and 6-31G(d) for other non-metal atoms [28-32] was denoted as BSI. Different singlet and multiplet states were clarified with B3LYP and ROB3LYP approaches including Becke's three-parameter hybrid functional combined with Lee−Yang−Parr correction for correlation [33,34]. The nature of each structure was verified by performing harmonic vibrational frequency calculations. Intrinsic reaction coordinate (IRC) calculations were examined to confirm the right connections among key transition-states and corresponding reactants and products. Harmonic frequency calculations were carried out at the B3LYP/BSI level to gain zero-point vibrational energy (ZPVE) and thermodynamic corrections at 353 K and 1 atm for each structure in MeOH. The solvation-corrected free energies were obtained at the B3LYP/6-311++G(d,p) (LanL2DZ for I) level by using integral equation formalism polarizable continuum model (IEFPCM) in Truhlar's "density" solvation model [35-37] on the B3LYP/BSI-optimized geometries.

As an efficient method of obtaining bond and lone pair of a molecule from modern ab initio wave functions, NBO procedure was performed with Natural bond orbital (NBO3.1) to characterize electronic properties and bonding orbital interactions [38,39]. The wave function analysis was provided using Multiwfn_3.7_dev package [40] including research on frontier molecular orbital (FMO) and Mayer bond order (MBO).

3 Results and Discussion

The mechanism was explored for PhI(OAc)$_2$-mediated Csp−Csp^2 bond cleavage of 1-alkynylnaphthol **1**, C=N/N−O bond cleavage of N-phenyl nitrone **2**, sequential recombination yielding [1,4]oxazinone **3** and bridged ring by-product **4** (Scheme 1). Illustrated by black arrow of Scheme 2, 1-alkynylnaphthol **1** was initially isomerized to VQM under base NEt$_3$, which underwent [4 + 3] cycloaddition with N-phenyl nitrone **2** affording intermediate **A**. Then 1,3-rearrangement of N−O vinyl group of **A** furnished intermediate **B**, the ring opening of which and sequential hydrogen shift gave iminium intermediate **C**. The intramolecular 1,4-addition of **C** delivered pyrroline intermediate **D**, of which the intermolecular alcoholysis with MeOH and PhI (OAc)$_2$ provided α-aminoketone intermediate **E** (red arrow). Then spirolactam **F** was formed via oxidative dearomatization of naphthol and intramolecular cyclization. Finally [1,4] oxazinone **3** was yielded in high diastereoselectivity from ring opening of **F** via intermediate **G** and sequential ester exchange via intermediate **H**. Alternatively, the intramolecular 1,2-addition of O-anion of **D** resulted in bridged ring by-product **4**, which could be transformed to **D** by hydrolysis (blue arrow).

The schematic structures of optimized TSs in Scheme 2 were listed by Figure 1. The activation energy was shown in Table 1 for all steps. Supplementary Table S1, Table S2 provided the relative energies of all stationary points. According to experiment, the Gibbs free energies in MeOH solution phase are discussed here.

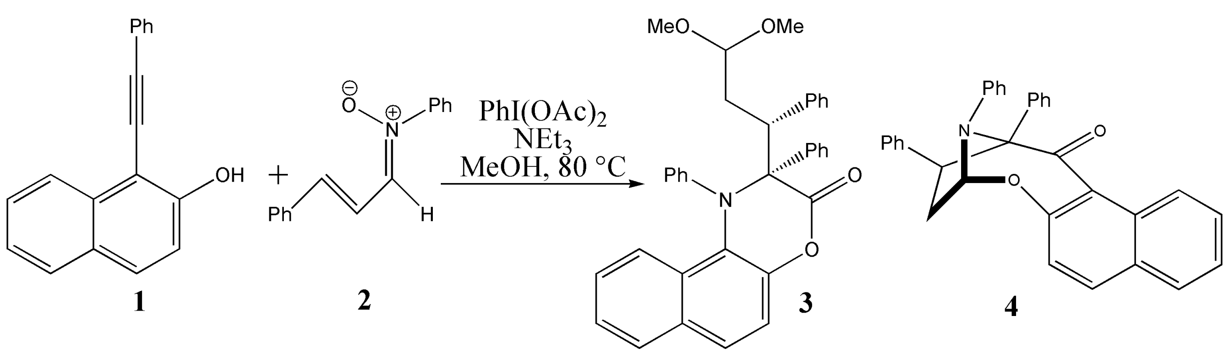

Scheme 1: PhI(OAc)$_2$-mediated Csp−Csp^2 bond cleavage of 1-alkynylnaphthol **1**, C=N/N−O bond cleavage of N-phenyl nitrone **2**, sequential recombination yielding [1,4]oxazinone **3** and bridged ring by-product **4**.

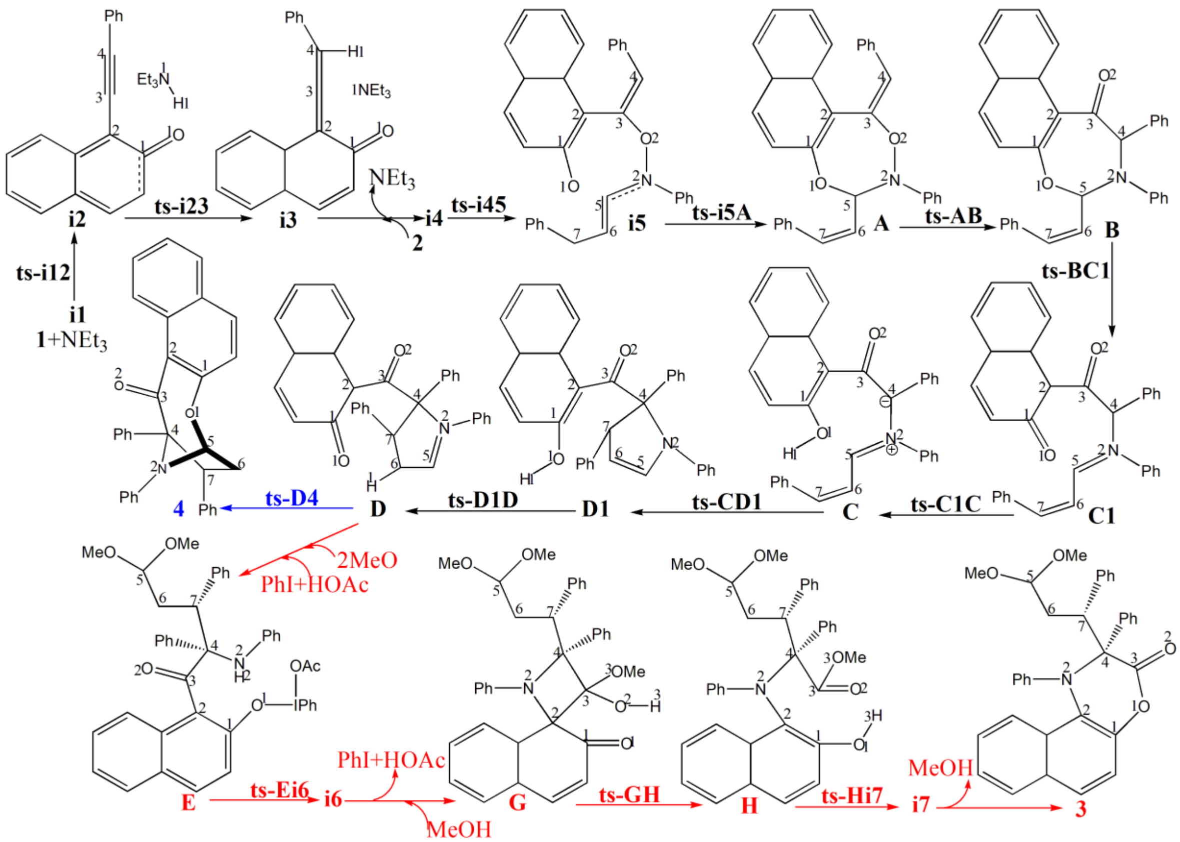

Scheme 2: Proposed mechanism of PhI (OAc)2-mediated Csp−Csp^2 bond cleavage of **1**, C=N/N−O bond cleavage of **2**, sequential recombination yielding **3** and **4**. TS is named according to the two intermediates it connects. TS is named according to the two intermediates it connects.

TS	$\Delta G^{\neq}_{gas}$	$\Delta G^{\neq}_{sol}$
ts-i12	23.6	21.3
ts-i23	11.1	12.3
ts-i45	13.4	11.7
ts-i5A	14.6	12.8
ts-AB	31.6	26.9
ts-BC1	27.2	22.9
ts-C1C	20.7	15.2
ts-CD1	29.8	25.8
ts-D1D	21.7	17.4
ts-D4	11.4	7.4
ts-Ei6	11.1	9.2
ts-GH	9.7	5.9
ts-Hi7	26.5	22.4

Table 1: The activation energy (in kcal mol^{-1}) of all reactions in gas and solvent

3.1 Isomerization of 1 to VQM with NEt₃

Under the assistance of base NEt_3, initial two steps are required for the isomerization of 1-alkynylnaphthol **1** to VQM. From complex **i1** between **1** and NEt_3, the proton of naphthol hydroxyl group is deprived by negative N of base via **ts-i12** in step 1 with the activation energy of 21.3 kcal mol^{-1} endothermic by 2.4 kcal mol^{-1} producing reactive **i2** with (black dash line of Figure 1a). The transition vector indicates proton H1 transfer from O1 to N1 (1.54, 1.36 Å). The C1-O1 is strengthened to be carbonyl group of VQM in **i2** along with sp3 hybrid N1 easy to hand over the proton to negative alkyne C4.

Therefore of via **ts-i23** in step 2 the proton H1 is shifting from N1 to C4 (1.29, 1.43 Å) with decreased activation energy of 12.3 kcal mol^{-1} exothermic by -4.2 kcal mol^{-1} generating stable **i3** binding VQM and recovered NEt_3. Not only includes proton transfer, the transition vector also suggests alkyne turning to be reactive conjugated diene (Figure S1a). Here NEt_3 functions as bridge transferring proton to facilitate two steps of isomerization.

(a)

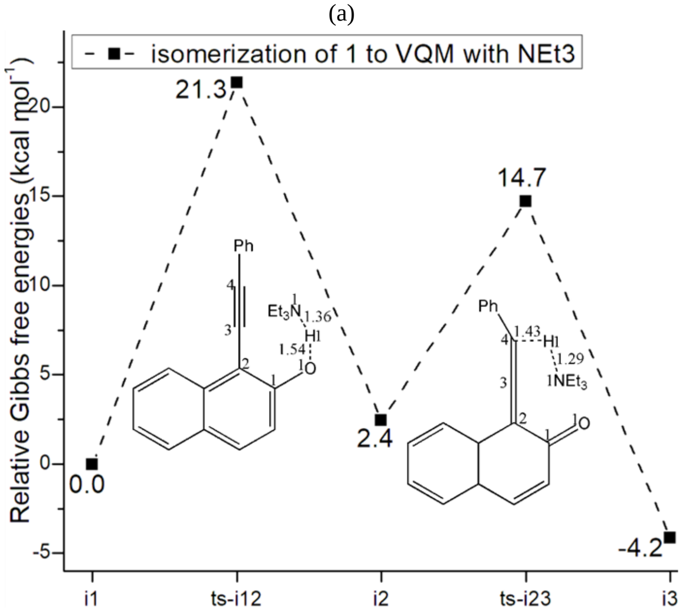

(b)

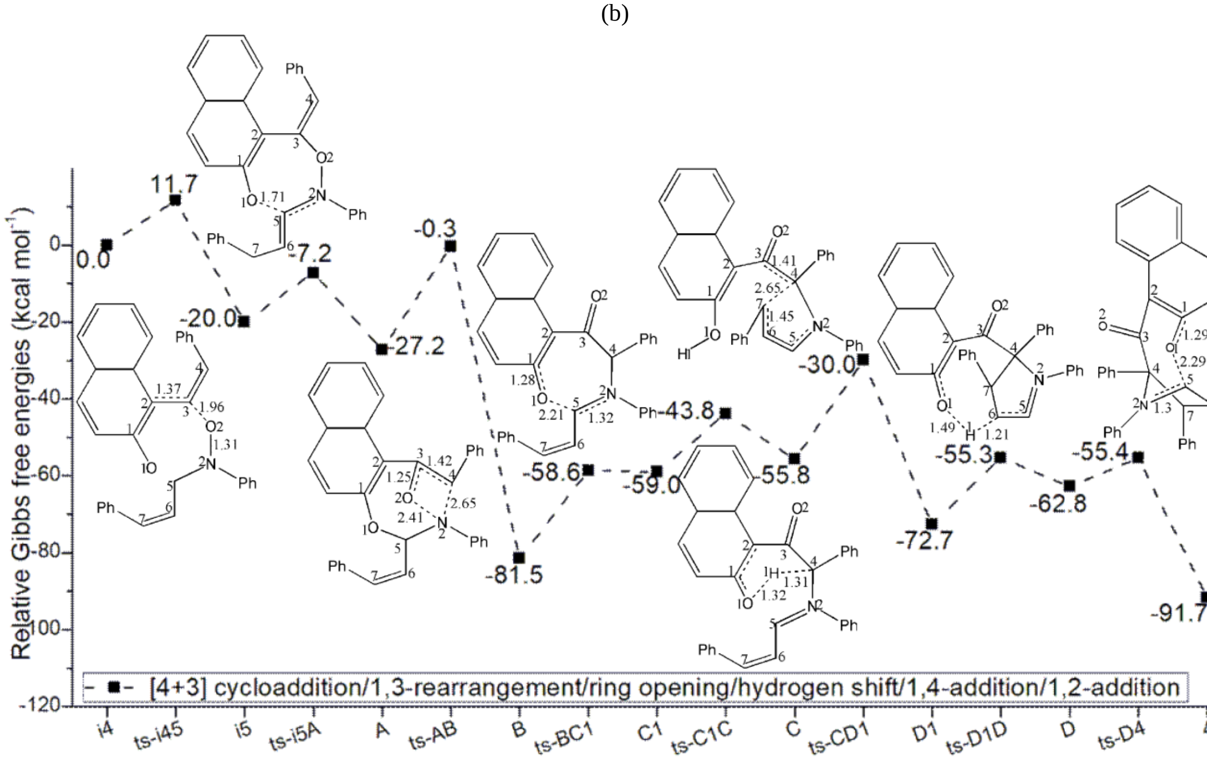

(c)

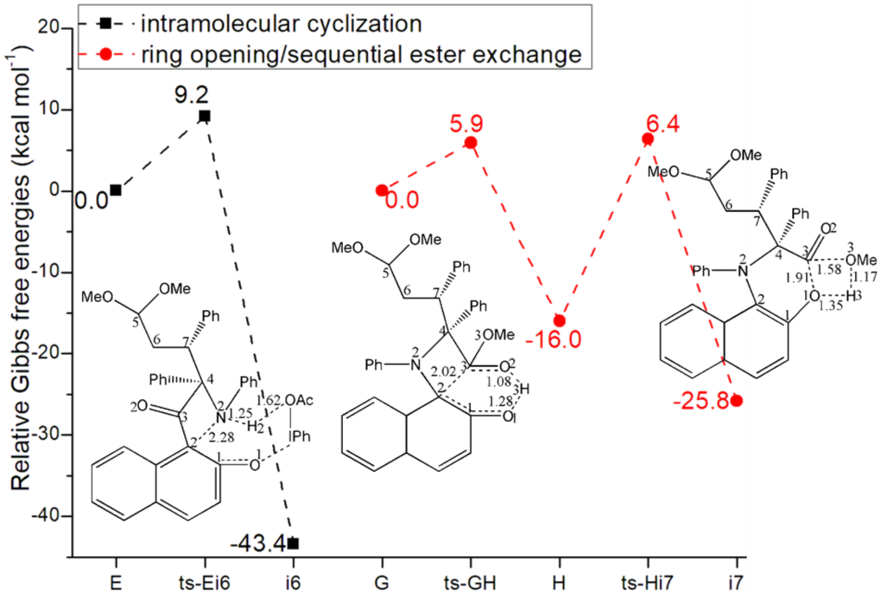

Figure 1: Relative Gibbs free energy profile in solvent phase starting from complex (a) **i1** (b) **i4** (c) **E, G** (Bond lengths of optimized TSs in Å).

3.2 [4+3] cycloaddition/N−O vinyl 1,3-rearrangement/ring opening/hydrogen shift/1,4-addition

Added with N-phenyl nitrone **2**, the complex denoted as **i4** is taken as starting point of the following seven steps (black dash line of Figure 1b). VQM undergoes [4 + 3] cycloaddition with **2** via **ts-i45** in step 3 with activation energy of 11.7 kcal mol^{-1} affording stable intermediate **i5** exothermic by -20.0 kcal mol^{-1}. The transition vector contains nucleophilic addition of O2 to C3 and the cooperative stretching of N2-O2, C3-C2 bond from double to single (1.96, 1.31, 1.37 Å) (Figure S1b). The next step 4 is required to realize the formation of seven-membered intermediate **A** via **ts-i5A** with activation energy of 12.8 kcal mol^{-1} continuously exothermic by -27.2 kcal mol^{-1}. The transition vector corresponds to the approaching of O1 to C5 (1.71 Å). In addition to typical O1-C5 single bond, the closure heptatomic ring **A** also involves C1-C2, C3-C4 conjugated double bond. Owing to the reactive VQM, both of the two steps are readily accessible in kinetics but favorable from thermodynamics.

Then 1,3-rearrangement of N−O vinyl group of **A** takes place via **ts-AB** in step 5 with activation energy of 26.9 kcal mol^{-1} greatly exothermic by -81.5 kcal mol^{-1} giving intermediate **B**. The transition vector is complicated with a series of atomic motions about cleavage of N2-O2, linkage of N2-C4 bond as well as shortened of C3-O2 from single to double while elongation of C3-C4 from double to single (2.41, 2.65, 1.25, 1.42 Å) (Figure S1c). Obviously, the structure of **B** is another heptatomic ring much more stable than **A** supporting 1,3-rearrangement of N−O bond, which is significant and determined to be rate-limiting from kinetics.

Subsequently, the ring opening of **B** occurs via **ts-BC1** with mediate activation energy of 22.9 kcal mol^{-1} exothermic by -59.0 kcal mol^{-1} in step 6 yielding **C1** involving increased relative energy of 22.5 kcal mol^{-1} compared with **B**. According to the transition vector, this process is composed of O1-C5 bond breaking along with contraction of C1-O1 and N2-C5 bond from single to double (2.21, 1.28, 1.32 Å) (Figure S1d). Hence a sequential hydrogen shift is easy via **ts-C1C** in step 7 with decreased activation energy of 15.2 kcal mol^{-1} exothermic by -55.8 kcal mol^{-1}. The transition vector reveals a proton transfer mode of C4···H1···O1 (1.31, 1.32 Å). An iminium intermediate **C** is furnished with positive N2 and negative charge focused on C4 ready to initiate the nucleophilic attack afterwards.

Next intramolecular 1,4-addition of **C** proceeds via **ts-CD1** in step 8 with activation energy of 25.8 kcal mol^{-1} generating stable **D1** followed by proton transfer via **ts-D1D** in step 9 with reduced activation energy of 17.4 delivering pyrroline intermediate **D** exothermic by -62.8 kcal mol^{-1}. The transition vector suggests nucleophilic addition of C4···C7, stretching C3···C4, C6···C7 (2.65, 1.41, 1.45 Å) (Figure S1e) and then O1···H1···C6 (1.49, 1.21 Å). Finally, the stable pentacyclic alkene **D1** with C5=C6 double bond turns to be pyrroline **D** with N2=C5 and sp3 hybrid C6. With relative energy uphill by 9.9 kcal mol^{-1} from **D1**, **D** is more likely to trigger subsequent processes.

3.3 O-anion 1,2-addition or intramolecular cyclization/ring opening/sequential ester exchange

Two feasible paths are located for the formation of two products. On one hand, the intramolecular 1,2-addition of O-anion of **D** takes place via **ts-D4** in step 10 with activation energy of 7.4 kcal mol^{-1} delivering bridged ring by-product **4**, which could be transformed to **D** by hydrolysis. The transition vector corresponds to a process just reverse to that of **ts-BC1** comprising O1-C5 bonding together with extension of C1-O1 and N2-C5 bond from double to single (2.29, 1.29, 1.30 Å). The new seven membered oxygen heterocyclic ketone is obtained in **4** fused with previous five membered nitrogen heterocyclic ring.

Alternatively, with additional MeOH and $PhI(OAc)_2$, the intermolecular alcoholysis of **D** could provide α-aminoketone intermediate **E** (black dash line of Figure 1c). The intramolecular cyclization happens via **ts-Ei6** in step 11 with activation energy of 9.2 kcal mol^{-1} exothermic by -43.4 kcal mol^{-1} resulted in quaternary nitrogen heterocyclic ketone **i6**. The transition vector contains detailed atomic motion about nucleophilic addition of negative N2 to C2 and depriving proton H2 from N2 by OAc (2.28, 1.25, 1.62 Å). Via oxidative dearomatization, spirolactam **F** is given after the removal of PhI and HOAc from **i6**.

Then another MeOH molecule is added to C3=O2 of **F** in forms of MeO and H making it to be C3-O2 single one and sp3 hybrid C3 in **G**, which is located as new starting point of last two steps (red dash line of Figure 1c). Via **ts-GH**, the ring opening proceeds in step 12 with low activation energy of 5.9 kcal mol^{-1} exothermic by -16.0 kcal mol^{-1} yielding intermediate **H**. This process is illustrated according to the transition vector composed of C3-C2 dissociation and proton shift O2···H3···O1 in concerted mode (2.02, 1.08, 1.28 Å) (Figure S1f). There are also cooperated exchange of C3-O2 and C1-O1 beween double and single.

Finally, a sequential ester exchange takes place from **H** via **ts-Hi7** with mediate activation energy of 22.4 kcal mol^{-1} exothermic by -25.8 kcal mol^{-1} yielding intermediate **i7** in last step 13. As shown by the transition vector, this process is collaborative yet asynchronous with proton transfer O1⋯H3⋯O3 in front and nucleophilic attack of O1 to C3 as well as resultant O3 cleavage from C3 behind (1.35, 1.17, 1.91, 1.58 Å) (Figure S1g). Once O1-C3 is bonded in **i7**, a new hexacyclic lactone is realized not only with recovered MeOH but producing [1,4]oxazinone **3** with high diastereoselectivity.

The relative energy of **4** higher by 28.5 kcal mol^{-1} than that of **3** is in accordance with **4** as by-product and major one **3** in experiment [22]. To highlight the idea of feasibility for changes in electron density and not molecular orbital interactions are responsible of the reactivity of organic molecules, quantum chemical tool Multiwfn was applied to analyze of electron density such as MBO results of bonding atoms and contribution of atomic orbital to HOMO of typical TSs (Table S3, Figure S2). These results all confirm the above analysis.

4 Conclusions

Our DFT calculations provide the first theoretical investigation on iodine(III)-mediated selective Csp−Csp^2 bond cleavage of 1-alkynylnaphthol with N-phenyl nitrone. Under base NEt_3, 1-alkynylnaphthol was isomerized to VQM, which underwent [4 + 3] cycloaddition with N-phenyl nitrone affording heptatomic ring. Then 1,3-rearrangement of N−O vinyl group was determined to be rate-limiting furnishing another heptatomic ring much more stable, the ring opening of which and sequential hydrogen shift gave iminium intermediate. The intramolecular 1,4-addition delivered pyrroline through pentacyclic alkene intermediate. The intermolecular alcoholysis with MeOH and $PhI(OAc)_2$ provided α-aminoketone intermediate. Via oxidative dearomatization and intramolecular cyclization, spirolactam was formed followed by ring opening and ester exchange producing major product [1,4]oxazinone with high diastereoselectivity. Alternatively, the intramolecular 1,2-addition of O-anion resulted in bridged ring by-product. The lower yield of by-product is induced by higher relative energy than major one. The positive solvation effect is suggested by decreased absolute and activation energies in MeOH solution compared with in gas. These results are supported by Multiwfn analysis on FMO composition of specific TSs, and MBO value of vital bonding, breaking.

Electronic Supplementary Material

Supplementary data available: [Computation information and cartesian coordinates of stationary points; Calculated relative energies for the ZPE-corrected Gibbs free energies (ΔG_{gas}), and Gibbs free energies (ΔG_{sol}) for all species in solution phase at 353 K.]

Author contributions: Conceptualization, Nan Lu; Methodology, Nan Lu; Software, Nan Lu; Validation, Nan Lu; Formal Analysis, Nan Lu; Investigation, Nan Lu; Resources, Nan Lu; Data Curation, Nan Lu; Writing-Original Draft Preparation, Nan Lu; Writing-Review & Editing, Nan Lu; Visualization, Nan Lu; Supervision, Chengxia Miao; Project Administration, Chengxia Miao; Funding Acquisition, Chengxia Miao. All authors have read and agreed to the published version of the manuscript.

Funding: This work was supported by National Natural Science Foundation of China (21972079) and Key Laboratory of Agricultural Film Application of Ministry of Agriculture and Rural Affairs, P.R. China.

Conflict of interest: The authors declare no conflict of interest.

References

1. Li, E.-Q.; Lindsley, C. W.; Chang, J.; Yu, B. (2024). Molecular Skeleton Editing for New Drug Discovery. *J. Med. Chem*. 67, 13509-13511.
2. Liu, S.; Yang, Y.; Song, Q.; Liu, Z.; Lu, Y. et al. (2024). Tunable molecular editing of indoles with fluoroalkyl carbenes. Nat. *Chem*. 16, 988-997.
3. Song, F.; Wang, B.; Shi, Z.-J. (2023). Transition-Metal-Catalyzed C−C Bond Formation from C−C Activation. Acc. *Chem*. Res. 56, 2867-2886.
4. Shi, S.-H.; Liang, Y.; Jiao, N. (2021). Electrochemical Oxidation Induced Selective C−C Bond Cleavage. *Chem*. Rev. 121, 485-505.
5. Zhou, P.; Wang, J.-Y.; Zhang, T.-S.; Li, G.; Hao, W.-J. et al. (2018). Thiazolium salt-catalyzed C−C triple bond cleavage for accessing substituted 1-naphthols via benzannulation. *Chem. Commun*. 54, 164-167.
6. Wang, P.-L.; Shen, H.-Z.; Cheng, H.-H.; Gao, H.; Li, P.-H. (2020). Electrochemical esterification reaction of alkynes with diols via cleavage of carbon−carbon triple bonds without catalyst and oxidant. *Green Chem*. 22, 6783-6791.
7. He, F.-S.; Yao, Y.; Xie, W.; Wu, J. (2020). Metal-Free Synthesis of (E)-Vinyl Sulfones via An Insertion of Sulfur Dioxide/1,5-Hydrogen Atom Transfer Sequence. Adv. Synth. Catal. 362, 4744-4748.
8. Takano, H.; Okazaki, S.; Nishibe, S.; Ito, T.; Shiozawa, N. et al. (2020). Gold-catalyzed dual C−C bond cleavage of biphenylenes bearing a pendant alkyne at ambient temperature. Org. Biomol. *Chem*. 18, 5826-5831.
9. Qin, C.; Feng, P.; Ou, Y.; Shen, T.; Wang, T. et al. (2013). Selective C sp 2 -C sp Bond Cleavage: The Nitrogenation of Alkynes to Amides. Angew. Chem., Int. Ed. 52, 7850-7854.
10. Gaydou, M.; Echavarren, A. M. (2013). Gold-Catalyzed Synthesis of Tetrazoles from Alkynes by C-C Bond Cleavage. Angew. Chem., Int. Ed. 52, 13468-13471.
11. Qin, W.; Liu, Y.; Yan, H. (2022). Enantioselective Synthesis of Atropisomers via Vinylidene ortho-Quinone Methides (VQMs). Acc. Chem. Res. 55, 2780-2795.
12. Guo, W.-T.; Zhu, B.-H.; Chen, Y.; Yang, J.; Qian, P.-C. et al. (2022). Enantioselective Rh-Catalyzed Azide-Internal-Alkyne Cycloaddition for the Construction of Axially Chiral 1,2,3-Triazoles. *J. Am. Chem*. Soc. 144, 6981-6991.
13. Zhang, X.; Li, S.; Yu, W.; Xie, Y.; Tung, C.-H. et al. (2022). Asymmetric Azide−Alkyne Cycloaddition with Ir(I)/Squaramide Cooperative Catalysis: Atroposelective Synthesis of Axially Chiral Aryltriazoles. *J. Am. Chem*. Soc. 144, 6200-6207.
14. Luo, Y.; Lu, Y.-J.; Pan, M.-M.; Liang, Y.-F.; Shi, W.-M. et al. (2024). Rapidly diastereoselective assembly of ten-membered N-heterocycles between two 1,3-dipoles and their diversity to access fused N-heterocycles. *Chin. Chem*. Lett. 110207.
15. Xu, Y.; Gao, H.-X.; Pan, C.; Shi, Y.; Zhang, C. et al. (2023). Stereoselective Photoredox Catalyzed (3 + 3) Dipolar Cycloaddition of Nitrone with Aryl Cyclopropane. Angew. Chem, Int. Ed. 62, No. e202310671.
16. Zhou, S.; Li, Y.; Liu, X.; Hu, W.; Ke, Z. et al. (2021). Enantioselective Oxidative Multi-Functionalization of Terminal Alkynes with Nitrones and Alcohols for Expeditious Assembly of Chiral α-Alkoxy-β-amino-ketones. *J. Am. Chem*. Soc. 143, 14703-14711.
17. Li, M.-F.; Shi, S.-Q.; Xu, T.; Zhang, Q.; Hao, W.-J. et al. (2023). Stereoselective construction of azepine-containing bridged scaffolds via organocata-lytic bicyclization of yne-

allenone esters with nitrones. Chin. Chem. Lett. 34, 107751.

18. Li, T.-Z.; Liu, S.-J.; Sun, Y.-W.; Deng, S.; Tan, W. et al. (2021). Regio- and Enantioselective (3 + 3) Cycloaddition of Nitrones with 2-Indolylmethanols Enabled by Cooperative Organocatalysis. Angew. Chem., Int. Ed. 60, 2355-2363.
19. Wang, Y.; Yu, J.-N.; Wang, Y.; Shi, F. (2024). Intermolecular α-Functionalization of Benzylamides with N-Nucleophiles via Oxidative Umpolung: Synthesis of Tetrasubstituted 3,3′-Oxindoles. Org. Lett. 26, 6041-6046.
20. Wang, Y.; Yin, J.-C.; Zhang, Y.-W.; Zhang, Y. et al. (2024). Hypervalent iodine-mediated regioselective dearomatization of non-activated arenes. Adv. Synth. Catal. 366, 4253-4259.
21. Wei, C.; Zhou, Z.; Pang, G.-L.; Liang, C.; Mo, D.-L. (2022). Cinchonidine-Catalyzed Synthesis of Oxazabicyclo [4.2.1] nonanones from N-Aryl-α, β-unsaturated Nitrones and 1-Ethynylnaphthalen-2-ols. Org. Lett. 24, 4104-4108.
22. Zhao, Y.; Yan, L.-B.; Liao, L.-F.; Wu, G.-Q. et al. Nitrogenation of Alkynes with Nitrones to Prepare Functionalized [1,4]Oxazinones through Csp−Csp 2 Bond Cleavage. https://doi.org/10.1021/acs.orglett.4c03553
23. Kourounakis, A. P.; Xanthopoulos, D.; Tzara, A. (2020). Morpholine as a privileged structure: A review on the medicinal chemistry and pharmacological activity of morpholine containing bioactive molecules. Med. Res. Rev. 40, 709-752.
24. Arshad, F.; Khan, M. F.; Akhtar, W.; Alam, M.; Nainwal, M. L. M. et al. (2019). Revealing quinquennial anticancer journey of morpholine: A SAR based review. *Eur. J. Med. Chem*. 167, 324-356.
25. Tian, L.; Feng, H.; Dai, Z.; Zhang, R. (2021). Resorufin-based responsive probes for fluorescence and colorimetric analysis. *J. Mater. Chem*. B, 9, 53-79.
26. Frisch, M. J.; Trucks, G. W.; Schlegel, H. B. et al. (2010). Gaussian 09 (Revision B.01), Gaussian, Inc., Wallingford, CT.
27. Hay, P. J.; Wadt, W. R. (1985). Ab initio effective core potentials for molecular calculations-potentials for the transition-metal atoms Sc to Hg. *J. Chem. Phys*. 82, 270-283.
28. Lv, H.; Han, F.; Wang, N.; Lu, N.; Song, Z. (2022). Ionic Liquid Catalyzed C-C Bond Formation for the Synthesis of Polysubstituted Olefins. *Eur. J. Org. Chem*. e202201222.
29. Zhuang, H.; Lu, N.; Ji, N.; Han, F.; Miao, C. (2021). Bu4NHSO4-Catalyzed Direct N-Allylation of Pyrazole and its Derivatives with Allylic Alcohols in Water: A Metal-free, Recyclable and Sustainable System. Advanced Synthesis & Catalysis, 363, 5461-5472.
30. Lu, N.; Lan, X.; Miao, C.; Qian, P. (2020). Theoretical investigation on transformation of Cr(II) to Cr(V) complexes bearing tetra-NHC and group transfer reactivity. *Int. J. Quantum Chem*. 120, e26340.
31. Lu, N.; Liang, H.; Qian, P.; Lan, X.; Miao, C. (2020). Theoretical investigation on the mechanism and enantioselectivity of organocatalytic asymmetric Povarov reactions of anilines and aldehydes. *Int. J. Quantum Chem*. 120, e26574.
32. Lu, N.; Wang, Y. (2023). Alloy and Media Effects on the Ethanol Partial Oxidation Catalyzed by Bimetallic Pt6M (M= Co, Ni, Cu, Zn, Ru, Rh, Pd, Sn, Re, Ir, and Pt). Computational and Theoretical Chemistry, 1228, 114252.
33. Catellani, M.; Mealli, C.; Motti, E.; Paoli, P.; Perez-Carren˜o, E. et al. (2002). Palladium-Arene Interactions in Catalytic Intermediates: An Experimental and Theoretical Investigation of the Soft Rearrangement between η1 and η2 Coordination Modes. J. AM. CHEM. SOC. 124, 4336-4346.
34. Marenich, A. V.; Cramer, C. J.; Truhlar, D. G. (2009). Universal Solvation Model Based on Solute Electron Density and on a Continuum Model of the Solvent Defined by the Bulk Dielectric Constant and Atomic Surface Tensions. J. Phys. Chem. B, 113, 6378–6396.
35. Tapia, O. (1992). Solvent effect theories: Quantum and classical formalisms and their applications in chemistry and biochemistry. *J. Math. Chem*. 10, 139-181.
36. Tomasi, J.; Persico, M. (1994). Molecular Interactions in Solution: An Overview of Methods Based on Continuous Distributions of the Solvent. Chem. Rev. 94, 2027-2094.
37. Tomasi, J.; Mennucci, B.; Cammi, R. (2005). Quantum Mechanical Continuum Solvation Models. Chem. Rev. 105, 2999-3093.
38. Reed, A. E.; Weinstock, R. B.; Weinhold, F. (1985). Natural population analysis. *J. Chem. Phys*. 83, 735-746.
39. Reed, A. E.; Curtiss, L. A.; Weinhold, F. (1988). Intermolecular interactions from a natural bond orbital donor-acceptor view point. Chem. Rev. 88, 899-926.
40. Lu, T.; Chen, F. (2012). Multiwfn: A multifunctional wavefunction analyzer. J. Comput. Chem. 33, 580-592.

This work is licensed under Creative Commons Attribution 4.0 License

To Submit Your Article Click Here: **Submit Manuscript**

DOI:10.31579/2690-4861/632

Ready to submit your research? Choose Auctores and benefit from:

- fast, convenient online submission
- rigorous peer review by experienced research in your field
- rapid publication on acceptance
- authors retain copyrights
- unique DOI for all articles
- immediate, unrestricted online access

At Auctores, research is always in progress.

Learn more https://auctoresonline.org/journals/international-journal-of-clinical-case-reports-and-reviews